Journal of Non-Crystalline Solids 355 (2009) 1760–1768

Contents lists available at ScienceDirect

Journal of Non-Crystalline Solids

journal homepage: www.elsevier.com/locate/jnoncrysol

# Method to assess the homogeneity of partially crystallized glasses: Application to a photo-thermo-refractive glass

Julien Lumeau [a,*], Alexander Sinitskii [a], Larissa Glebova [a], Leonid B. Glebov [a], Edgar D. Zanotto [b]

[a] CREOL/The College of Optics and Photonics, University of Central Florida, 32816 Orlando, FL, USA
[b] Vitreous Materials Laboratory, LaMaV, Department of Materials Engineering, DEMa, Federal University of São Carlos, UFSCar, 13.565-905 São Carlos, SP, Brazil

ARTICLE INFO

*Article history:*
Received 11 July 2008
Available online 24 July 2009

*PACS:*
61.43.Fs
42.70.Ce
78.20.Ci
61.82.Rx
68.55.Ac

*Keywords:*
Crystallization
Glass ceramics
Optical microscopy
Photoinduced effects
Calorimetry

ABSTRACT

We describe a new method for the study of both optical and crystallization homogeneity of partially crystallized glasses or glass–ceramics at different spatial scales (from 100 mm to 1 μm). The method relies on the association of different techniques, such as interferometry, optical microscopy and differential scanning calorimetry. The method was tested to probe the optical and crystallization homogeneity of both as-made and UV-exposed, and pre-nucleated samples of a photo-thermo-refractive (PTR) glass. This study demonstrates that pure UV-exposure did not lead to an improvement of the crystallization homogeneity of the glass. However, the benefit of associating UV-exposure and nucleation thermal treatment was clear. These combined treatments permit to homogenize the crystal distribution in PTR glass at millimeter and micron scale. This result is of major commercial interest.



## 1. Introduction

Photo-thermo-refractive (PTR) glass is a photosensitive glass that undergoes significant refractive index changes after successive UV-exposure and thermal development [1–4] which is due to the precipitation of nanosize crystals in the UV-exposed areas. Therefore, this glass is suitable for phase hologram recording and is attractive for many advanced applications, such as optical filtering, mode selection in lasers and spectral beam combining [5,6]. PTR glass is a sodium–potassium–zinc–aluminum–silicate glass containing fluorine and bromine, doped with cerium, silver, antimony and tin. Glasses which undergo photo-thermo-induced crystallization were invented many years ago by Stookey [7] and have been studied as possible candidates for hologram writing in the last 20 years [1–4]. After exposure of this glass to UV-radiation followed by thermal development [8] crystallization of up to 3 wt% sodium fluoride nanocrystals occurs and the net result is a decrease of the local refractive index in the UV-exposed crystallized regions. An early description of the complex photo-thermo-induced crystallization mechanisms of PTR glass is given in Ref. [9]. To be used as an optical component, PTR glass must have excellent transmission (more than 99% for a few millimeters thick sample) in the 400–2000 nm range after thermal development, hence only a small volume fraction of nanosize NaF crystals is allowed.

Several important aspects of PTR glass technology motivated the study of its homogeneity. First of all, the manufacturing of good quality optical glass, especially in small scale, is very challenging. Therefore, the homogeneity of refractive index over the whole melt must be measured and characterized. The homogeneity of refractive index is directly associated to the average chemical homogeneity of the glass. Moreover, PTR glass being photosensitive, its homogeneity also requires homogeneity of photosensitivity (i.e. the distribution of nanocrystals within the UV-exposed areas of heat-treated glass must be extremely uniform). This uniformity is determined by the spatial distribution of certain elements that control crystal nucleation. However, these elements represent only a tiny fraction of the glass. To be more precise, two very important components present in the glass, *fluorine* and *bromine*, play a key role in both optical and crystallization homogeneity. As these two elements are highly volatile, it is very complicated to precisely control their concentration and spatial distribution in the glass. Moreover, it was shown in Refs. [10,11] that bromine has a significant impact on the nucleation of PTR glass. It was also

* Corresponding author. Tel.: +1 321 948 5115.
*E-mail address:* jlumeau@creol.ucf.edu (J. Lumeau).

0022-3093/$ - see front matter © 2009 Elsevier B.V. All rights reserved.
doi:10.1016/j.jnoncrysol.2009.05.054

demonstrated that bromine-free PTR glass does not show any DSC crystallization peak below 720 °C, and even a pre-nucleation treatment does not contribute to crystallization in such Br-depleted glass, i.e. a DSC crystallization peak is absent (but appears in Br-containing PTR glass). As fluorine is necessary for the formation of sodium fluoride crystals, it is obvious that its concentration plays a key role on the crystallization process. In addition to Na, F and Br, four dopants: cerium, silver, antimony, and tin are likely to be involved in the nucleation process. Hence, a systematic study of the *crystallization homogeneity* (controlled by the spatial uniformity of Na, F, Br and *dopants*) and of *optical homogeneity* (controlled by the spatial uniformity of the major constituents of the glass) is necessary for an exhaustive analysis of the overall homogeneity of PTR glass.

The use of PTR glass for the fabrication of holographic optical elements requires high homogeneity of refractive index and of photosensitivity. While homogeneity of refractive index is a traditional parameter for the certification of optical materials, homogeneity of photosensitivity in inorganic glasses has not yet been dealt with. In this paper, the homogeneity of both *refractive index* and *crystallization* is characterized at different scales (from 100 mm to 1 μm) by associating different techniques, such as interferometry, optical microscopy, and differential scanning calorimetry (DSC). We first characterize the homogeneity of virgin PTR glasses and then study and discuss the effect of UV-exposure and successive UV-exposure and pre-nucleation heat-treatment on PTR glass homogeneity.

## 2. Experimental description

### 2.1. Glass sample preparation

Several photosensitive glasses of nominal composition $15Na_2O$–$5ZnO$–$4Al_2O_3$–$70SiO_2$–$5NaF$–$1KBr$–$0.01Ag_2O$–$0.01CeO_2$ (mol%) doped with Sn and Sb were studied in this work. The glasses were melted in an electrical furnace in a 1 L platinum crucible at 1460 °C for 5 h. Stirring was employed to homogenize the melt. After melting, the glasses were cooled in air down to the glass transition temperature, then annealed at 460 °C for 2 h, and finally cooled down to room temperature at 0.1 °C/min. Several polished samples of $2 \times 25 \times 25$ mm$^3$ were prepared from each melt. Based on spectro-photometric measurements (absorption at 3 μm), fluctuations of OH content were estimated to be within 10% in all glass melts.

### 2.2. Interferometry

The *optical homogeneity* of each sample was tested by the shadow method in the divergent beam of a He–Ne laser (decimeter scale). With this method, optical heterogeneities results in a distortion of the projected beam and, therefore, striae can be located in the glass. To properly quantitate the *optical homogeneity* a commercial Zygo interferometer was used. Mapping of the local refractive index variation over the whole sample surface was carried out for each sample, and the value of the peak-to-valley refractive index heterogeneity was measured. This technique was thus used to probe the overall chemical homogeneity at millimeter scale.

### 2.3. Non-isothermal DSC measurements

Thermal analyses were performed on bulk samples using a Q10 calorimeter from TA instruments with a typical weight of 30 mg and a heating rate of 30 °C/min under argon atmosphere. Due to the limited temperature range of our DSC equipment, spectra were measured only up to 720 °C. For simplicity we only show the spectra in the range 450–720 °C. Only one exothermic peak could be seen in each thermogram, thus the positions of their maxima were taken as the "DSC crystallization temperature" of each sample ($T_c$). This technique was used to probe the *crystallization homogeneity* at millimeter scale (mm size monolithic samples).

### 2.4. Optical microscopy

Images of crystal distributions were performed with a Zeiss optical microscope and objectives from 20× to 100×. To be able to use this technique, some samples were *hyper-developed* for 30 min at 650 °C to achieve micron size crystals (commercial PTR glass as used for optical applications has nanosize crystals). Moreover, due to the opacity of the samples resulting from excessive crystallization at 650 °C, the microscope was used in reflection mode. Finally, crystal counting statistics were performed directly on the micrographs. This technique was used to probe the PTR *crystallization homogeneity* at micron scale (dimension of the areas probed by optical microscopy).

## 3. Results

### 3.1. Homogeneity of as-made PTR glasses at centimeter scale

#### 3.1.1. Homogeneity from melt to melt

The study at *centimeter scale* of PTR glass homogeneity consisted in characterizing the evolution of the crystallization temperature of virgin (unexposed, unheated) PTR glasses from melt to melt. Non-isothermal DSC measurements were carried out on samples from several different melts and the DSC crystallization temperature was determined on each thermogram. Table 1 summarizes the results. This experiment demonstrates that $T_g$ is almost the same for all tested samples, from different melts, but $T_c$ presents large variations, from 660 °C to higher than 720 °C! This most interesting fact will be discussed later in this article.

#### 3.1.2. Homogeneity within a melt

The second step of this study consisted in measuring the variation of the crystallization temperature within a melt. Melt 1 was cut into 20 different slices, from bottom to top. From each slice one $25 \times 25$ mm$^2$ sample was cut and polished, and the *chemical homogeneity* (indirectly determined by refractive index variations) was checked with a Zygo interferometer to eliminate parts containing striae corresponding to refractive index fluctuations over a few tens of ppm. Two corners of each sample were then cut and analyzed in the DSC. Due to the high crystallization temperature of this particular melt (which is outside the measurable range of our DSC), the samples were nucleated for 20 min at 495 °C to shift the crystallization peak to a lower temperature [11]. Then, non-isothermal DSC measurements were carried out on each sample and the respective crystallization temperatures were measured. Fig. 1 shows the evolution of the crystallization temperature along the glass melt cylinder axis, for each corner. This experiment demonstrates that large variations of the crystallization temperature, as high as 50 °C, appear in different samples from a single melt.

We also studied the evolution of the crystallization temperature in the radial direction in the glass melt cylinder. In order to avoid any thermal treatment, we have chosen a melt that presented a

**Table 1**
DSC crystallization temperature from melt to melt.

| Glass | Melt 1 | Melt 2 | Melt 3 | Melt 4 | Melt 5 | Melt 6 | Melt 7 |
|---|---|---|---|---|---|---|---|
| $T_g$ (°C) | 498.0 | 499.7 | 498.8 | 500.7 | 501.2 | 498.9 | 498.5 |
| $T_c$ (°C) | >720 | 705 | 671 | 703 | 666 | 652 | 680 |

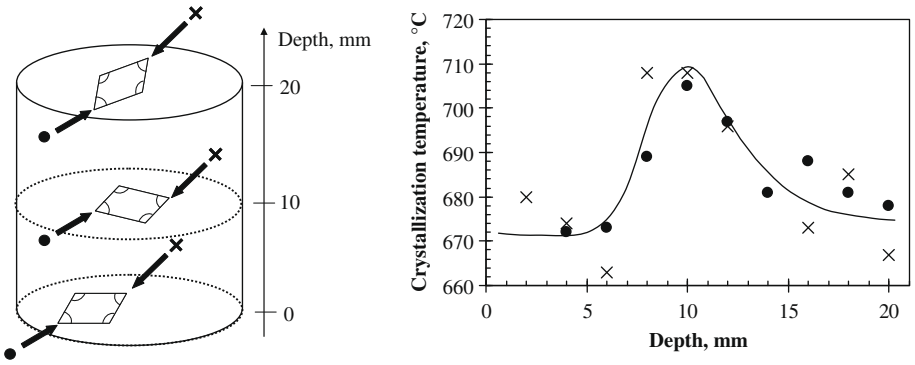


**Fig. 1.** DSC crystallization temperature for PTR glass samples from melt 1, pre-nucleated for 20 min at 495 °C, as a function of the vertical position of the sample in the melt – homogeneity at centimeter scale.

relatively low crystallization temperature (melt 7 of Table 1). Non-isothermal DSC measurements were carried out using small ($\sim 2 \times 2 \times 2$ mm$^3$) samples taken from one edge to another of the melt along the diameter, all samples being separated by 15 mm. Fig. 2 shows the evolution of the measured crystallization temperature as a function of sample position. This experiment demonstrates once more that the crystallization temperature varies significantly, from 655 to 705 °C according to the sample position in the melt. It is important to note that sample 6 was very close to a stria (very large compositional variation) and this fact may explain why no crystallization peak appears.

### 3.1.3. Influence of the chemical homogeneity on the crystallization temperature

The last step of the study of homogeneity at *large scale* consisted in trying to associate the average crystallization temperature (i.e. the crystallization temperature observed for most of the melt) with the average optical homogeneity of the melt. Between 20 and 30, $25 \times 25 \times 5$ mm$^3$ specimens were cut from melts 2 and 6 (these samples represent almost all that can be made from a 800 g melt). Each specimen was checked with the shadow method and no visible heterogeneity could be seen. With our shadow setup the sensitivity limit corresponds to variation of refractive index smaller than about 200 ppm, peak-to-valley. This sensitivity is more than one order of magnitude lower than the one shown in Ref. [12] due to the use of an optimized design. Both sides of the samples were polished to better than $\lambda/5$ and their *optical homogeneity* was then precisely measured with the Zygo interferometer. Fig. 3 shows the *optical heterogeneity* as a function of sample number for each melt. It is very important to stress that no visible striae were present in each sample and, therefore, the measured values are typical of the real degree of homogeneity of the glass yield. Similar observations were made with other melts.

### 3.2. Homogeneity of as-made PTR glass at millimeter scale

The second step of the homogeneity study was carried out on $25 \times 25 \times 5$ mm$^3$ samples that were cut from melt 6. This melt was chosen due to its low temperature of non-isothermal crystallization, which can be measured without any pre-nucleation treatment. Moreover, as Fig. 3 shows, this glass presents very different degrees of homogeneity from one sample to another, and is thus interesting for our purpose.

#### 3.2.2. Homogeneous sample

The first experiment consisted of gauging the crystallization temperature of a sample showing very good *optical homogeneity* by the Zygo interferometer. A sample having maximum variation of refractive index of 54 ppm peak-to-valley – the largest part of

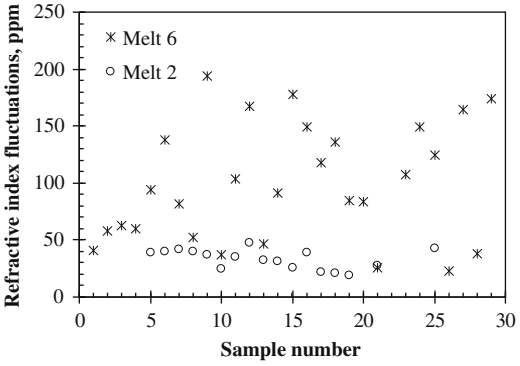


**Fig. 3.** Maximum peak-to-valley refractive index fluctuations measured by a Zygo interferometer for melts 2 and 6 – homogeneity at centimeter scale.

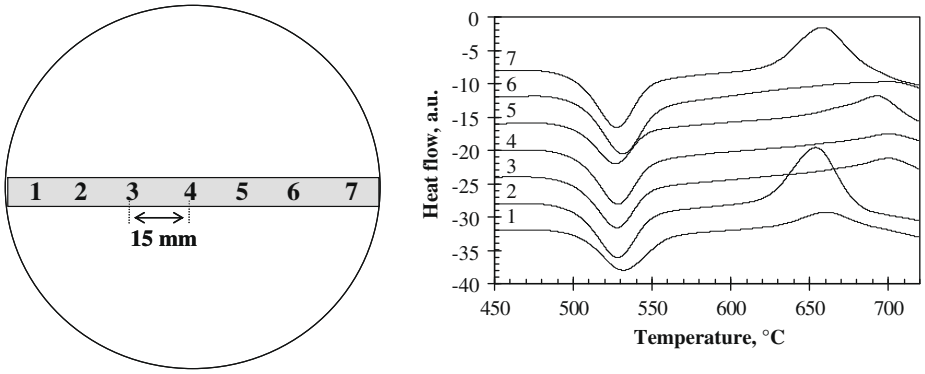


**Fig. 2.** DSC crystallization temperature for PTR glass from one slice of melt 7 as a function of the radial position of the sample in the melt – homogeneity at centimeter scale.

the sample having a degree of homogeneity less than 25 ppm – was chosen. A $2 \times 25 \times 5$ mm$^3$ slice was cut from one edge of the sample, and six $2 \times 4 \times 5$ mm$^3$ samples were cut from this slice. Each sample was therefore very homogeneous. Then non-isothermal DSC measurements were carried out. Fig. 4 shows the thermogram for each sample. Whatever the sample, the crystallization temperature is about 652 ± 2 °C.

*3.2.3. Heterogeneous sample*

The second step consisted in studying a glass that showed a higher degree of heterogeneity but no visible striae. Thus a glass sample having maximum refractive index variation of 190 ppm was chosen. Mapping of the refractive index fluctuations over the sample surface was performed with the Zygo interferometer. Several $5 \times 5 \times 2$ mm$^3$ samples originating from several parts of that sample and having distinct refractive indices were cut and non-isothermal DSC measurements were carried out on each sample. Fig. 5 presents the thermograms for the different samples. First of all, this experiment demonstrates that even at smaller scale, the crystallization temperature, $T_c$, can vary significantly. In this case, the fluctuations of $T_c$ are about 50 °C. To further illustrate this difference, isothermal DSC runs carried out at 580 °C showed that glasses having lower crystallization temperature crystallize 4× faster than glasses having higher crystallization temperatures. Based on the mapping of the local refractive index fluctuations and the precise knowledge of the position of each measured sample within the glass melt, we were also able to associate the crystallization temperatures to local refractive index fluctuations. Fig. 6 shows that this sample presents two widely different crystallization temperatures: 697 ± 2 °C for the regions where the refractive index ($n$) is the lowest ($n < n_0 - 75$ ppm, where $n_0$ is the average refractive index of the glass sample) and 652 ± 2 °C for the regions where refractive index is the highest ($n > n_0 + 100$ ppm). Between these two values of refractive index fluctuation, the crystallization temperature shows a sharp variation from 697 to 652 °C.

*3.3. Homogeneity of as-made PTR glass at micron scale*

*3.3.1. Heterogeneous sample*

The next step of our survey consisted in studying homogeneity at *micron scale* by direct crystal counting. A $5 \times 5 \times 25$ mm$^3$ slice cut from a sample of melt 6 was chosen. Then a Zygo image was taken and maximum refractive index fluctuations of about 140 ppm were measured. Finally this sample was hyper-developed for 4 h at 650 °C. Such long thermal treatment was performed to grow crystals to diameters large enough to be visualized with an optical microscope. Then the surface of each sample was repolished. However we have demonstrated that, during thermal development, a depletion of fluorine occurs on the sample surface as result of the high volatility of fluorine. To illustrate this problem, we first looked with the microscope at a polished edge of the sample after repolishing its top surface. In this way we demonstrated that a 15 μm layer without any visible crystals appears at this edge (Fig. 7). Chemical analysis carried out by Secondary Ion Mass Spectrometry (SIMS) demonstrated that this layer corresponds to a fluorine depleted layer, and consequently, a layer having very low concentration of sodium fluoride crystals. Then for this sample we recorded different micrographs at different parts of the sample showing clearly different refractive indices (Fig. 8). The micrographs show that crystallization kinetics are totally different

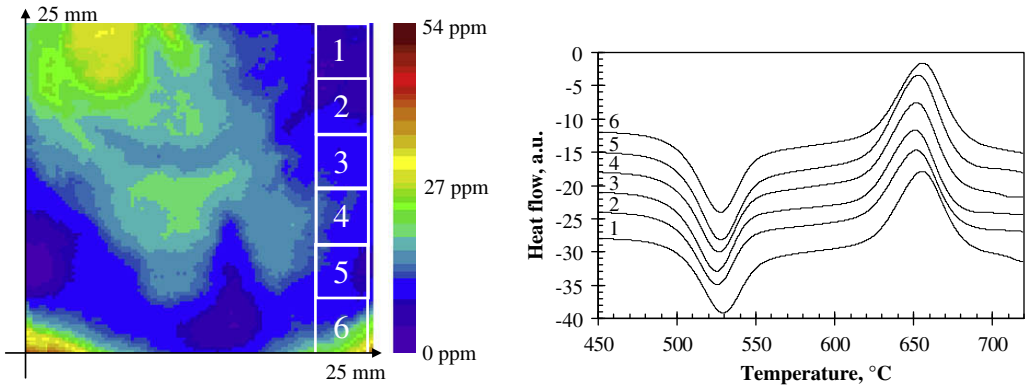


**Fig. 4.** Evolution of DSC crystallization temperature of a homogeneous sample issued from melt 6 as a function of sample position – homogeneity at millimeter scale.

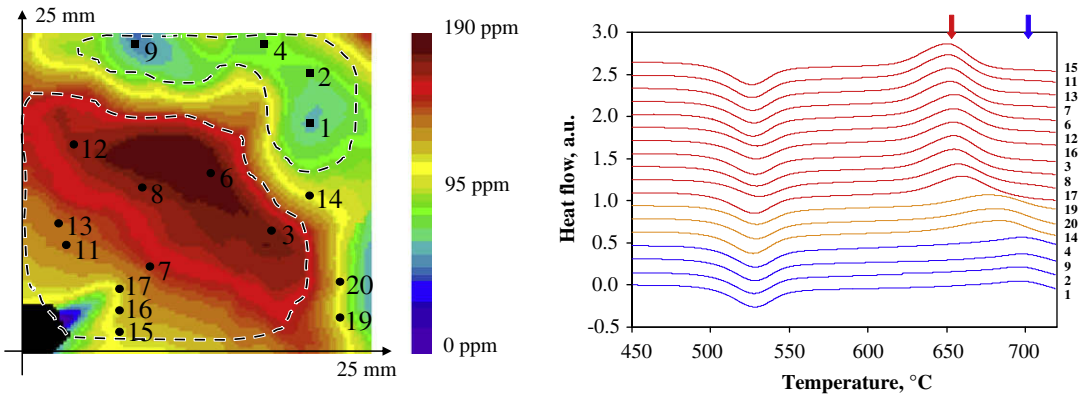


**Fig. 5.** Evolution of crystallization temperature measured by DSC of a heterogeneous sample from melt 6 as a function of sample position – homogeneity at millimeter scale.

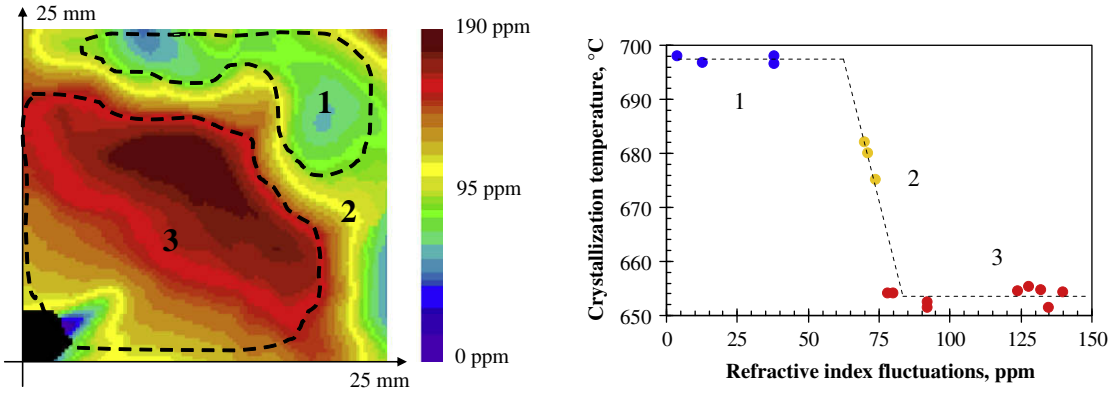


**Fig. 6.** Crystallization temperature measured by DSC of a heterogeneous sample from melt 6 as a function of refractive index variations determined by Zygo – homogeneity at millimeter scale.

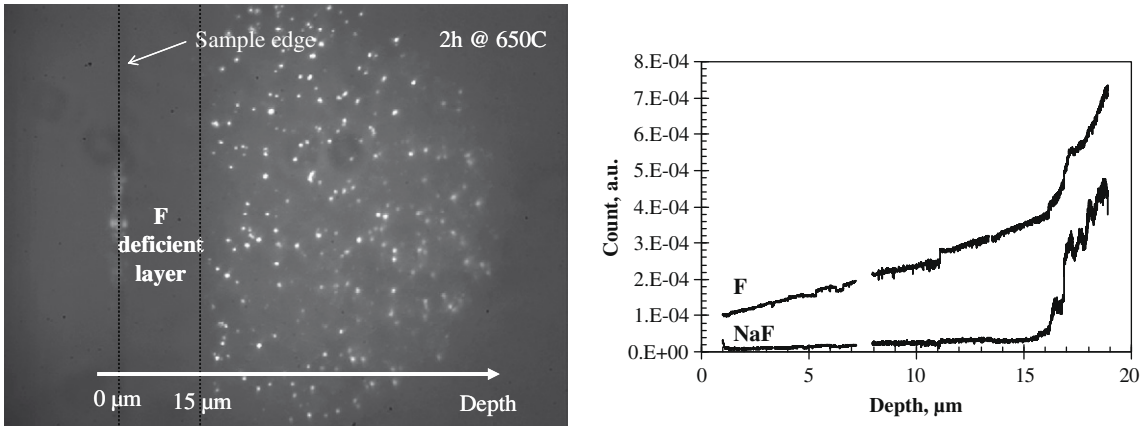


**Fig. 7.** Micrograph showing the depleted F layer on the surface of PTR glass after hyper-thermal development – homogeneity at micron scale.

according to the refractive index and chemical composition: the area having the lowest refractive index has a lower number of large crystals, and the area having the highest refractive index has a higher number of small crystals. Therefore, as expected, chemical composition plays an important role on the nucleation process.

*3.3.2. Crystallization statistics method*

It was recently demonstrated [13] that it is possible to gauge the *crystallization homogeneity* of a glass by performing a crystallization statistics analysis. The proposed method is based on the fact that for a certain nucleation time at a given temperature, each volume element of a homogeneous glass has the same probability to nucleate a crystal. Due to the stochastic nature of this phenomenon, the probability $p(N_{vi})$ of finding $N_{vi}$ nuclei in a volume $V_i$ is given by a Poisson law:

$$p(N_{vi}) = \frac{N_v^{N_{vi}} e^{-N_{vi}}}{N_{vi}!}, \tag{1}$$

where $N_v$ is the average number of crystals in that particular volume. If the average number of crystals per examined field and the corresponding standard deviation ($\sigma_N$) can be determined, and if the condition of random volume distribution is met and follows Poisson's statistics, then the average number of crystals and its associated standard deviation will be linked by the following relationship:

$$\sqrt{N_v} = \sigma_N. \tag{2}$$

Thus, it is possible to estimate the homogeneity of the glass by plotting a curve of $\sigma_N/N_v$ versus $1/N_v^{0.5}$ and to compare the position of the measured point to the expected Poisson line. If the slope of the straight line crossing the origin and the measured data is equal to 1, then the glass is considered perfectly homogeneous (a Poisson glass). Then, any point that is over this slope 1 line corresponds to a heterogeneous glass. In addition, the largest the distance from this line, the higher the degree of heterogeneity.

*3.3.3. Crystallization statistics results*

We applied this technique for the characterization of samples having different degrees of heterogeneity. We took five samples ($25 \times 25 \times 5$ mm$^3$) of melt and measured the optical heterogeneity of each sample. One sample showed a relatively high degree of heterogeneity (~140 ppm), another sample showed a low degree of heterogeneity (~30 ppm), and the remaining three had a moderate degree of heterogeneity of about ~70 ppm. It is important to stress that the degree of homogeneity found in most of PTR glass samples is orders of magnitude higher than any regular glass made in laboratory scale.

Then these samples were hyper-developed for 4 h at 650 °C, repolished, and several optical micrographs were taken from different parts of each sample. Typical number of pictures taken for each sample was 15–20, and number of crystals in each picture was between 100 and 400. The number of crystals on each micrograph was precisely counted, and the average number of crystals and its standard deviation were calculated for each sample and added in the $\sigma_N/N_v$ versus $1/N_v^{0.5}$ plot (Figs. 9 and 10). First of all,

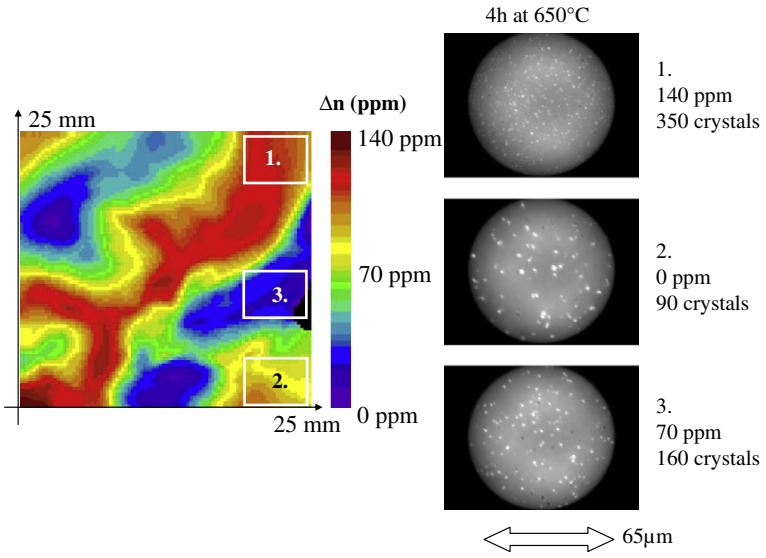


**Fig. 8.** Micrographs recorded at different positions of a heterogeneous PTR glass sample from melt 6 after hyper-thermal development – homogeneity at micron scale.

the glass presenting the highest optical heterogeneity (140 ppm) is the farthest from the Poisson line. Then the three intermediate samples (70 ppm of refractive index variation) are close, but somewhat above the Poisson line. Also the datum for the glass showing the lowest optical heterogeneity (30 ppm) is situated under the Poisson line.

Finally, in order to have an idea of the glass optical homogeneity in another scale, we also calculated the corresponding average value and standard deviation of optical heterogeneity (in ppm) of melts 2 and 6 using the results of Fig. 3. Then the corresponding points were added in the graph in Fig. 9. At that scale, therefore, the lower the heterogeneity of the associated point, the closer it lies to the Poisson line.

### 3.4. Homogeneity of UV-exposed PTR glass

The same technique used to gauge the homogeneity at different scales of virgin glass was applied to test the homogeneity of UV-exposed glass.

#### 3.4.1. Homogeneity of millimeter scale

Samples from melt 6 were chosen and UV-exposed with a Helium–Cadmium laser (325 nm, 4 mW). Previous studies [4] indicated that 0.9 J/cm$^2$ is an optimum dosage to achieve high refractive index changes and low optical losses for efficient hologram writing. Each sample was exposed to that optimum UV-dosage and the optical heterogeneities of the glass were mapped with the Zygo interferometer before and after exposure (but no changes were observed) and DSC spectra were then taken for each glass. The thermograms showed that the crystallization temperatures of UV-exposed glasses shift to low temperatures by a few degrees compared to virgin glasses. However, in the case of heterogeneous glasses, the same wide range of crystallization temperatures (~50 °C) as those obtained with virgin glass were observed in UV-exposed glasses. Therefore, the crystallization homogeneity at millimeter scale *is not affected* by UV-exposure and hence is the same for virgin and UV-exposed PTR glasses.

#### 3.4.2. Homogeneity at micron scale

Some samples were used for DSC measurements and the other part of the same samples was hyper-developed for 4 h at 650 °C. Then these samples were repolished and optical micrographs were recorded. The images demonstrate that UV-exposure has an important effect: the number of nucleation centers increases compared to non-exposed glasses. However, in terms of crystallization statistics, very similar results were found in UV-exposed and non-exposed glasses, i.e. the homogeneity of crystallization at micron

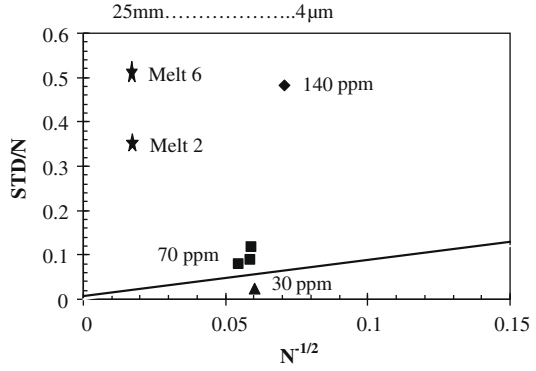


**Fig. 9.** Crystal statistics carried out on samples from melt 6 having different degrees of heterogeneity. Calculated average number of crystals ($N_v$) and standard deviation ($\sigma_N$) in a $\sigma_N/N_v$ versus $1/N_v^{0.5}$ plot, and comparison of the position of these points with expected Poisson statistics (solid line).

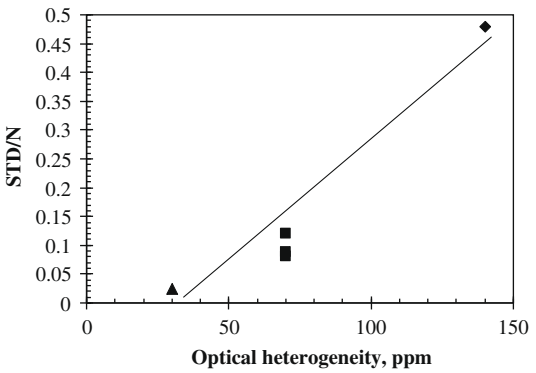


**Fig. 10.** $\sigma_N/N_v$ ratio at constant $1/N_v^{0.5}$ as a function of refractive index heterogeneity.

scale is essentially not affected by UV-exposure and is the same for virgin and UV-exposed PTR glasses.

### 3.5. Homogeneity of UV-exposed and pre-nucleated PTR glasses

The last step of this study was to gauge the homogeneity of UV-exposed and pre-nucleated PTR glass samples. It was previously demonstrated [11] that the association of UV-exposure and pre-nucleation permits to lower the DSC crystallization temperature. Therefore, we studied the influence of this treatment on the homogeneity of PTR glasses.

#### 3.5.1. Homogeneity at millimeter scale

We cut another stripe from the same slice of melt 7, which was used for the radial homogeneity study of virgin glass (Section 3.1), tangential to the stripe that was used before and which presented different crystallization temperatures. As this slice was unpolished, the level of heterogeneity could not be measured using the Zygo interferometer, but was estimated to be ~150–200 pm. This stripe was UV-exposed with a dosage of 0.9 J/cm$^2$ and nucleated for 30 min at 510 °C. Non-isothermal DSC measurements were then carried out on small pieces issued from this stripe, each sample being separated by 15 mm and tangential to the samples that were used for the study of the homogeneity of virgin PTR glass. Fig. 11 shows the measured crystallization temperature as a function of sample position (to be compared with Fig. 2). Except for sample 6, the main crystallization peak is centered at 600 ± 1 °C. Sample 6 has a crystallization peak centered at 605 °C, which is very close to the crystallization temperature of each sample. This small difference comes from the fact that this sample was taken from an area close to a striae. However, this experiment clearly demonstrates that this double treatment (UV-exposure and pre-nucleation) somehow homogenizes the crystallization temperature of the glass. Finally, it is very important to note that all DSC thermograms are almost identical, and therefore, not only the crystallization temperature, but the whole thermogram becomes the same for each piece.

#### 3.5.2. Homogeneity at micron scale

Lastly we studied the impact of successive UV-exposure and pre-nucleation treatments of PTR glass on the homogeneity at micron scale. We took the same slice of melt 7 that was used for the homogeneity study at millimeter scale, and which was UV-exposed and nucleated for 30 min at 510 °C. Then this sample was hyper-developed for 4 h at 650 °C. Finally, the sample was repolished and microscope pictures were taken at different areas of the sample. A total of 10–15 micrographs were taken, each micrograph having about 400 crystals. The number of crystals on each micrograph was counted and the average number and standard deviation were then calculated and plotted on a $\sigma_N/N_v$ versus $1/N_v^{0.5}$ plot (Fig. 12). This experiment demonstrates that UV-exposure and nucleation permitted to highly improve the micron-scale *homogeneity of crystallization* of PTR glasses. Moreover, this point is situated almost on the slope 1 curve. This result means that quite uniform and random crystallization occurred in this glass and that the association of UV-exposure and pre-nucleation permitted to obtain a glass that can now be considered as homogeneous as a "Poisson glass".

## 4. Discussion

Homogeneity at large scale of virgin (i.e. unexposed and untreated glass) PTR glass was first studied. We have shown that large fluctuations of the crystallization temperature could be seen from melt to melt (Table 1). It is important to recall that this glass contains 16 components, including fluorine and bromine, which are highly volatile. Hence, their concentration in the final glass is very difficult to precisely control. Moreover, these components were demonstrated to play a key role on the crystallization process [10,11]. Therefore, this first result confirms the sensitivity of the crystallization process of PTR glass on minor compositional variations.

The scale was then decreased and the homogeneity of PTR glass was studied within one liter melts by non-isothermal DSC (Figs. 1 and 2). The axial homogeneity was first tested and it was demonstrated that crystallization varies by over 50 °C from edge to center. Moreover, this evolution is not random, but follows a smooth evolution; $T_c$ is much higher in the center of the glass cylinder than on the edge. It could be first thought that this change of crystallization temperature is due to the gradient of temperature that appears during the PTR glass cooling (the temperature is expected to be higher over longer durations in the center of the melt rather than on the edge), which would result in the creation of a higher number of nuclei in the center than on the edge. Then, this effect should result in a lower temperature of crystallization in the center of the melt than on the edge. However, this supposition is in contradiction with the data shown in Fig. 1. Moreover, the higher crystallization temperature in the center of the melt is confirmed by the study of the axial homogeneity of PTR glass (Fig. 2). Thus this result signs to a variation of some of the chemical elements, most probably fluorine and bromine. However, these are very light elements and their concentrations are very low; therefore, no reliable chemical analysis could determine the local concentration of these species and to correlate with optical and crystallization properties. Finally, complementary experiments with another slice did not show any significant axial change (in most of it) of crystallization temperature. Therefore, the crystallization homogeneity of PTR glass at large (cm) scale is difficult to control.

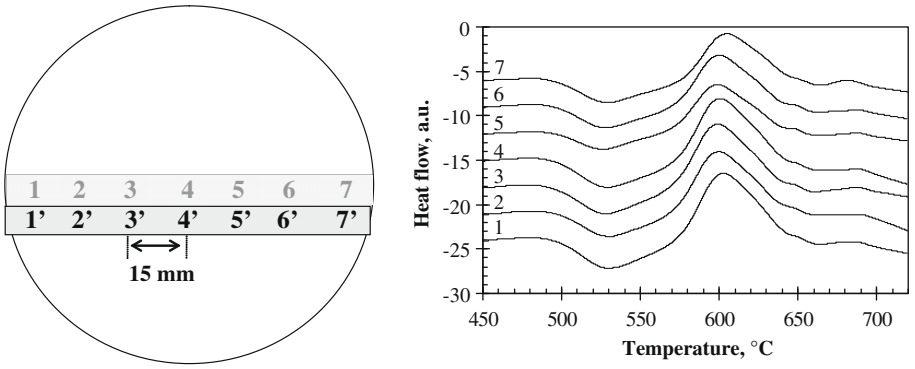


**Fig. 11.** DSC spectra measured on different parts of melt 7 that were successively UV-exposed and pre-nucleated 30 min at 510 °C – homogeneity at millimeter scale.

A very interesting feature of the PTR glass homogeneity was shown in Fig. 3. In this case optical homogeneity was measured in a glass having different average crystallization temperatures. We have shown that homogeneity is an order of magnitude higher in the glass having the largest crystallization temperature. Hence, this result demonstrates that there is a direct link between the crystallization temperature and the homogeneity of the whole melt.

After the above detailed study of the homogeneity of PTR glass at large (centimeter) scale, the homogeneity at millimeter scale was tested. We tested the possible correlation between crystallization temperature (as measured by non-isothermal DSC) and chemical homogeneity (Figs. 4–6). We demonstrated that a detectable uniform crystallization temperature can be found only in glasses presenting very low fluctuation of refractive index. Glasses presenting fluctuations of refractive index of more than 100 ppm will result in large fluctuations of the crystallization temperature. The most striking result is that this crystallization temperature varies sharply by 50 °C within a minor change of the refractive index of 20 ppm! But as it was shown in Ref. [10], small fluctuations of bromine content can dramatically change the crystallization behavior of PTR glass. Regarding fluorine, it is obvious that changes in its concentration will have a direct impact on PTR glass crystallization since it is part of NaF crystals, but it will also have an impact on the glass refractive index, since atomic refraction of NaF is about 1.3, while the one of $Na_2O$ is 1.6 [14]. In other words, this result corroborates the idea that variations of crystallization temperature from part to part of a glass sample are closely linked to chemical heterogeneity.

The last step consisted in studying the evolution of the homogeneity of as-made PTR glass at micron scale. In Fig. 8, the dependence of the crystal density and size on the local refractive index was shown. It was demonstrated that hyper-development of area with the highest refractive index will result in the appearance of the highest crystal density and the smallest crystal diameter. This effect relies on the fact that a maximum of ~2 mol% of sodium fluoride crystals can precipitate in PTR glass due to the limited amount of fluorine. This remark has a strong consequence because crystallization in PTR reaches saturation as soon as there is no fluorine available. Therefore, it can be seen that the final crystal size is closely linked to the number of nucleation centers sites. As observed in these micrographs, an increase of crystal number density is generally accompanied by a decrease of crystal size. Also, it is seen that, as expected, if a glass shows a low DSC crystallization temperature (area of largest refractive index in Fig. 6), it will also result in the presence of a larger number of nuclei and therefore a larger number of crystals (area of largest refractive index in Fig. 8).

After correlating the refractive index with the crystallization temperature, the crystal density or number we correlated the crystallization homogeneity with the optical homogeneity. Fig. 9 shows the evolution of the crystallization statistics parameters for glasses presenting different degrees of homogeneity. It can be seen that the lower the refractive index fluctuation the closer the respective point to the Poisson curve and, therefore, the higher the glass homogeneity. But, to perform a complete analysis of the homogeneity of our glass, it is important to recall that the amount of fluorine that acts in the crystallization process is only a few percent. Therefore, every time a crystal precipitates and grows a depletion of F and Na in the surrounding zone happens, and this phenomenon hinders the nucleation of new crystals in the F and Na depleted area. In this particular case (of depletion), it is possible to show that crystal statistics of a homogeneous glass is not described by the Poisson law and the corresponding experimental point in the $\sigma_N/N_v$ versus $1/N_v^{0.5}$ plot is under the slope 1 straight line. Hence, for PTR glass, a very homogeneous glass, the ($\sigma_N/N_v$, $1/N_v^{0.5}$) dot

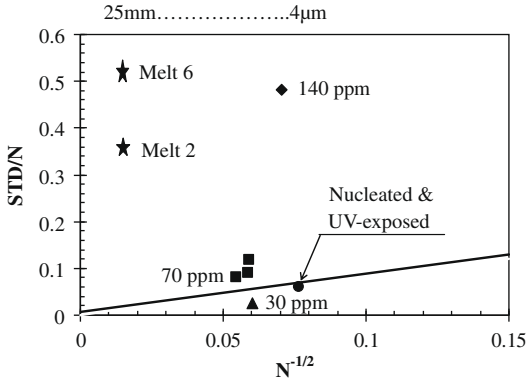


**Fig. 12.** Crystal statistics carried out on samples from melt 7 having different degrees of heterogeneity and which were successively UV-exposed and pre-nucleated 30 min at 510 °C. Calculated average number of crystals and standard deviation in a $\sigma_N/N_v$ versus $1/N_v^{0.5}$ plot and comparison of the position of these points with Poisson statistics.

is below the slope 1 line. Such a behavior can be observed for the glass having the highest homogeneity (Fig. 9). Fig. 10 shows how the $\sigma_N/N_v$ ratio evolves almost linearly with the optical heterogeneity ($\Delta n$). In other words, there is a quasi-linear relationship between the optical heterogeneity and the crystallization heterogeneity.

After studying the homogeneity of as-made PTR glass, we studied the effect of UV-exposure and pre-exposure on PTR glass homogeneity. However, we did not find any significant effect of UV-exposure on the crystallization homogeneity of PTR glass; while UV-exposure associated with pre-nucleation induces a very significant improvement of the homogeneity of PTR glass at all scales, as can be seen in Figs. 11 and 12. After UV-exposure associated with a proper pre-nucleation, the statistical parameters of a glass presenting chemical heterogeneity plotted on a $\sigma_N/N_v$ versus $1/N_v^{0.5}$ plot are situated below the Poisson curve. This result confirms the high improvement of the crystallization homogeneity of the glass.

It is important to recall once more that a maximum number of NaF crystals can precipitate due to the very limited amount of NaF in the original glass. Without UV-exposure and pre-nucleation, spontaneous *homogeneous* nucleation of NaF takes place in the bulk of the glass, but the number of nuclei and, therefore, the number of crystals that appear is far from reaching that maximum number. Hence, even small changes in the local chemical composition (Na, F...) may result in a large change in the number of crystals from one part to another of a given glass sample. On the other hand, by UV-exposing and pre-nucleating the glass, one induces copious *heterogeneous* nucleation on silver or AgBr particles, which precipitate in the glass, and thus come close to the saturation limit of nuclei that can be achieved in PTR glass. Therefore, crystallization is less sensitive to local changes of chemical composition. Moreover, the number of heterogeneous nuclei is related to the silver concentration in the original glass, which becomes metallic silver and *diffuses very fast* upon UV-exposure followed by pre-nucleation, and thus this concentration of silver is expected to become uniformly distributed in different parts of a given glass sample. Therefore, one can expect that these two effects result in better homogeneity of crystallization. While this homogenization of the crystallization properties of PTR glass occurs, the overall chemical homogeneity remains unchanged with UV-expose followed by nucleation treatment!

## 5. Conclusion

We proposed a new method to gauge, at different scales, the optical and crystallization homogeneity of photosensitive optical

glasses and tested it with a photo-thermo-refractive glass. This method is based on the association of different techniques: Zygo interferometry permits to map the evolution of the optical (average chemical) heterogeneity over the sample; while non-isothermal differential scanning calorimetry and optical microscopy permit to gauge the crystallization homogeneity at centimeter, millimeter and micron scales.

Quantitative characterization of crystallization homogeneity using Poisson statistics was confirmed. This method allowed us to obtain a direct quantitative evaluation of the *degree* and *scale* of the crystallization homogeneity in the glass.

All these techniques were combined to characterize the homogeneity of virgin and UV-exposed and thermally developed PTR glasses for the first time. This study demonstrates that whatever the scale, a significant degree of heterogeneity occurs in this complex glass (although PTR glass remains one of the most homogeneous at laboratory scale). Pure UV-exposure did not lead to any improvement of the crystallization homogeneity of the glass. But, the benefit of associating UV-exposure and pre-nucleation thermal treatment was clearly demonstrated. These combined treatments permit to homogenize the crystal distribution in this glass at both millimeter and micron scale. This result is of major interest because PTR glass is suitable for hologram writing based on the crystallization of sodium fluoride crystals. If adequate pre-nucleation thermal treatment is applied to UV-exposed PTR glasses, then the key glass parameter that defines the quality of the holograms is its optical/chemical homogeneity.

## Acknowledgements

This work was partially supported by DARPA contracts HR-01-1041-0004 and HR-0011-06-1-0010. EDZ acknowledges Brazilian agencies Capes, CNPq and Fapesp (07/08179-9) for funding the research work here reported. The authors are indebted to Dr. Miguel O. Prado (Argentina) for helpful discussions regarding the application of Poisson statistics to PTR glass. The authors also thank Mikhail Klimov (MCF/UCF) for the SIMS measurements.

## References

[1] V.A. Borgman, L.B. Glebov, N.V. Nikonorov, G.T. Petrovskii, V.V. Savvin, A.D. Tsvetkov, Sov. Phys. Dokl. 34 (1989) 1011.
[2] L.B. Glebov, N.V. Nikonorov, E.I. Panysheva, G.T. Petrovskii, V.V. Savvin, I.V. Tunimanova, V.A. Tsekhomskii, Sov. Phys. Dokl. 35 (1990) 878.
[3] L.B. Glebov, Glass Sci. Technol. 75 (C1) (2002) 73.
[4] Leonid Glebov, in: Proceedings SPIE, vol. 6545, 2007 (Paper 654507).
[5] L.B. Glebov, V.I. Smirnov, C.M. Stickley, I.V. Ciapurin, Proc. SPIE 4724 (2002) 101.
[6] Leonid B. Glebov, in: Proceedings SPIE, vol. 6216, 2006 (Paper 621601).
[7] S.D. Stookey, Indust. Eng. Chem. 41 (1949) 856.
[8] N.F. Borrelli, D.L. Morse, PA. Sachenik, US Patent 4,514,053, 30th April 1985.
[9] D. Stookey, G.H. Beall, J.E. Pierson, J. Appl. Phys. 49 (1978) 5114.
[10] L. Glebova, J. Lumeau, M. Klimov, E.D. Zanotto, L.B. Glebov, J. Non-Cryst. Solids 354 (2008) 456.
[11] J. Lumeau, A. Sinitskii, L. Glebova, L. Glebov, E. Zanotto, Phys. Chem. Glasses: Eur. J. Glass Sci. Technol. B 48 (4) (2007) 281 (August).
[12] J.S. Stroud, Opt. Eng. 42 (6) (2003) 1618.
[13] L.A. Souza, M.L.G. Leite, E.D. Zanotto, M.O. Prado, J. Non-Cryst. Solids 351 (46–48) (2005) 3579.
[14] J.H. Simmons, K.S. Potter, Optical Materials, Academic Press, 2000. p. 151.